Journal of Geophysical Research: Biogeosciences

RESEARCH ARTICLE
10.1029/2017JG004311

Special Section:
Biogeochemistry of natural organic matter

The Ephemeral Signature of Permafrost Carbon in an Arctic Fluvial Network

Travis W. Drake[1], François Guillemette[1,2], Jordon D. Hemingway[3], Jeffery P. Chanton[4], David C. Podgorski[1,5], Nikita S. Zimov[6], and Robert G. M. Spencer[1]

[1]National High Magnetic Field Laboratory Geochemistry Group and Department of Earth, Ocean and Atmospheric Science, Florida State University, Tallahassee, FL, USA, [2]Now at Research Center on Watershed—Aquatic Ecosystem Interactions (RIVE), University of Quebec at Trois-Rivieres, Trois-Rivieres, Quebec, Canada, [3]Department of Earth and Planetary Sciences, Harvard University, Cambridge, MA, USA, [4]Department of Earth, Ocean and Atmospheric Science, Florida State University, Tallahassee, FL, USA, [5]Now at Pontchartrain Institute for Environmental Sciences, Department of Chemistry, University of New Orleans, New Orleans, LA, USA, [6]North-East Science Station, Pacific Institute of Geography Russian Academy of Sciences, Chersky, Russia

Key Points:
- Bacterial respiratory isotopic signatures of carbon dioxide revealed a downstream gradient of dissolved organic carbon substrates
- In streams with diverse organic carbon sources, the isotopic signature of respiratory carbon dioxide sourced from permafrost is masked
- Aliphatic and nitrogen-containing dissolved organic matter was associated with the production of aged, permafrost-derived carbon dioxide

Supporting Information:
- Supporting Information S1
- Data Set S1

Correspondence to:
T. W. Drake,
draketw@gmail.com

Citation:
Drake, T. W., Guillemette, F., Hemingway, J. D., Chanton, J. P., Podgorski, D. C., Zimov, N. S., & Spencer, R. G. M. (2018). The ephemeral signature of permafrost carbon in an Arctic fluvial network. *Journal of Geophysical Research: Biogeosciences*, *123*, 1475–1485. https://doi.org/10.1029/2017JG004311

Received 14 NOV 2017
Accepted 8 APR 2018
Accepted article online 17 APR 2018
Published online 7 MAY 2018

Abstract Arctic fluvial networks process, outgas, and transport significant quantities of terrestrial organic carbon (C), particularly dissolved organic carbon (DOC). The proportion of permafrost C in these fluxes, however, is poorly constrained. A primary obstacle to the quantification of permafrost-derived DOC is that it is rapidly respired without leaving a unique tracer of its presence. In this study, we investigated the production of bacterial respiratory carbon dioxide (CO_2; measured as dissolved inorganic carbon; DIC) during maximum late-summer thaw in sites spanning a fluvial network (Kolyma Basin, Siberia) to assess whether the biodegradation of permafrost DOC could be detected by the presence of a persistent aged (^{14}C-depleted) signature on the DIC pool. Using Keeling plot interpretation of DIC produced in bioincubations of river water, we show that bacteria respire varying sources of DOC moving downstream through the fluvial network. Respiration of permafrost (production of aged CO_2) was only detected in heavily permafrost thaw influenced sites. In nonpermafrost thaw impacted sites, ambient DIC was modern (^{14}C-enriched), but rather than precluding the respiration of permafrost OC upstream, we suggest that ^{14}C-depleted DIC is overwhelmed by modern DIC. Investigation of dissolved organic matter composition via Fourier transform ion cyclotron resonance mass spectrometry highlighted that elevated levels of aliphatic and nitrogen-containing compounds were associated with the production of aged DIC, providing molecular-level insight as to why permafrost-derived dissolved organic matter is rapidly respired. Overall, results from this study demonstrate the difficulty of tracing inputs of a highly reactive substrate to systems with diverse organic matter sources.

1. Introduction

Arctic permafrost soils contain ~1,700 Pg of organic carbon (OC), nearly double the amount of carbon (C) in the modern atmosphere (Schuur et al., 2013; Tarnocai et al., 2009). Rising ambient air temperatures in the Arctic caused by ongoing global climate change threaten to thaw and mobilize this vast store of Pleistocene aged OC (Schuur et al., 2015). This temperature-induced degradation of permafrost occurs by a number of processes, including thermokarst formation, ice-wedge thaw, bank erosion, and the deepening of the seasonal active-layer (Schuur et al., 2008, 2013). As permafrost soils thaw and deepen, they become more porous, thereby increasing surface water infiltration, hydrologic flow paths, and residence times in the soil active layer (Guo et al., 2007; Striegl et al., 2005). Collectively, permafrost thaw releases previously frozen OC and increases the areal and temporal exchange between thawed soils and surface waters. As a result, pore and surface waters (fluvial networks, lakes, and coastal systems) become important processing pathways driving the fate of permafrost-derived OC as temperatures continue to rise in the Arctic.

Over the past decade, several studies have investigated the dynamics of permafrost-derived OC mobilization to fluvial networks. Early studies on large Arctic rivers suggested that little to no permafrost C was mobilized to major rivers, as they found no evidence of aged (^{14}C-depleted) C in the dissolved OC (DOC) fraction at the mouth of large Arctic Rivers (Neff et al., 2006; Raymond et al., 2007). More recently, incubation studies demonstrated high biolability of permafrost-derived DOC (Abbott et al., 2014; Vonk et al., 2013, 2015), which in turn led Mann et al. (2015) and Spencer et al. (2015) to test an alternative explanation. Specifically, if permafrost-derived DOC is highly biolabile, it will be consumed by microbial respiration in headwater streams before it

can be transported to larger rivers. Mann et al. (2015) demonstrated that microbial respiration is supported to a greater degree by progressively modern carbon downstream through an Arctic fluvial network. Spencer et al. (2015) showed that the aliphatic compounds, unique to permafrost thaw dissolved organic matter (DOM) within the Kolyma Basin, were consumed during 28-day bioincubations and that the remnant DOM chemically resembled what is found in the main stem of the Kolyma (a major Arctic River). Using recent estimates for rate of permafrost thaw and DOC yields from permafrost soils, another study calculated that aged DOC should be detectable at the mouths of large arctic rivers if permafrost carbon persists in fluvial networks (i.e., it is not subject to microbial or photooxidation; Drake et al., 2015). These studies collectively posit a "rapid loss" model for permafrost OC mobilized to aquatic networks, but they do not provide a salient approach to quantifying the process. Our study represents a first step toward addressing this knowledge gap of how to trace and account for biolabile C that is rapidly respired to CO_2 in headwater streams.

Evidence from the aforementioned incubation studies suggests that permafrost-derived DOC is indeed rapidly and preferentially utilized by microbes in low-order streams before it can be exported to larger tributaries or rivers. The addition of ^{14}C-depleted CO_2 from this respiration should shift the radiocarbon age of the bulk dissolved inorganic carbon (DIC) pool and potentially provide a stable downstream tracer of permafrost inputs in Arctic watersheds, provided that the subsidy of ^{14}C-depleted CO_2 is proportionately high enough to lower the bulk signature below the range for modern terrestrial C (e.g., 71.6 ± 170‰ for the Kolyma Basin; Mann et al., 2015). Additions of respiratory CO_2 from permafrost may also shift the $\delta^{13}C$-DIC signature of the bulk pool, since permafrost is more enriched (−26.3 ± 1.3‰) than contemporary terrestrial vegetation (−28.5 ± 2.0‰) and more depleted than autochthonous DOC (−19.8 ± 3.0‰) in the Kolyma Basin (Mann et al., 2015). In this study, we test the following hypotheses: (1) Preferential utilization of aged, permafrost-derived DOC in headwater streams will produce ancient ^{14}C-depleted DIC; (2) significant levels of permafrost OC respiration relative to total OC respiration will impart an aged DIC signature in low-order streams that is traceable downstream; (3) DIC produced via microbial respiration will be progressively younger and will have a more autochthonous isotopic signature moving downstream; and (4) the $\Delta^{14}C$ of respiratory DIC will be inversely related to the % permafrost C in the initial DOC; i.e., more permafrost-derived OC in the initial sample will result in more ^{14}C-depleted respiratory DIC. Testing these hypotheses provides much needed insight as to whether microbially respired permafrost OC is susceptible to venting as CO_2 to the atmosphere from Arctic fluvial networks.

2. Materials and Methods

2.1. Study Site

The Kolyma Basin is the largest watershed completely underlain by continuous permafrost on Earth. The permafrost soils in this region are part of the larger Yedoma complex which is composed primarily of Pleistocene-aged loess deposits (Zimov et al., 2006). These frozen, organic-rich soils contain 50–90% ice and approximately 1–5% C by mass (Tarnocai et al., 2009; Zimov et al., 2006). The late fall sampling period was chosen because active layer depths reach their maximum at this time of year, potentially thawing previously unfrozen permafrost (Schuur et al., 2008). Samples were collected in August and September of 2015 from 17 sites spanning the fluvial network of the Kolyma River Basin, Siberia (Figure 1). Sites were classified by their position in the watershed and by stream width in accordance with Mann et al. (2015) as permafrost thaw (Yedoma thaw), erosion streams, streams, tributaries, and main stem. Streams were classified as headwaters $<$5 m in width that drained lakes, tundra, or boreal landscapes. Tributaries were four larger rivers between 5 and 200 m in width that flowed directly into the Kolyma River. The main stem was the Kolyma River sampled near the city of Chersky. Erosion streams were distinguished by high turbidity ($>$100 Nephelometric Turbidity Units) and presence of active mechanical bank erosion. The permafrost thaw stream was sampled at a river cut bank at the well-studied site of Davanni Yar where a thawing ice-wedge complex immersed in permafrost generated a small stream.

2.2. Sample Collection

Water samples were collected from the thalweg of streams or rivers using a sterile 60-mL syringe affixed with a prerinsed 0.7-μm syringe filter. For DIC, the sampling syringe was inverted below the water surface to expel any air bubbles prior to injection of filtered water into preevacuated 20-mL borosilicate glass serum vials. At each site, 6 × 20-mL borosilicate glass serum vials were filled with 15 mL of water, three of which were

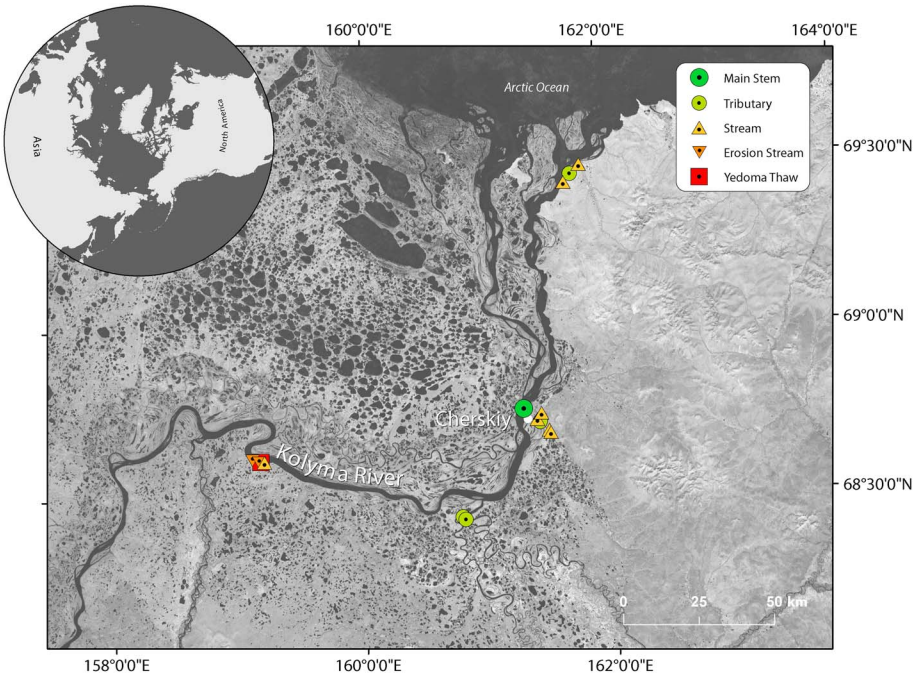

Figure 1. Study sites and sample locations by type.

acidified to pH ~2 with 1 mL of 30% H_3PO_4 immediately upon collection (t_0). The remaining three were incubated at room temperature for 28 days before acidification (t_{28}) to pH ~2 with 1 mL of 30% H_3PO_4. For DOC and DOM analyses, water samples were filtered through precombusted (450 °C $>$ 5 hr) Whatman GF/F filters into 125-mL acid-cleaned (10% HCl), triple-filtrate-rinsed HDPE bottles and preserved frozen until analysis.

Stream or river pH, temperature, specific conductivity, and dissolved oxygen were measured using a precalibrated YSI Pro-Plus handheld sonde. CO_2 partial pressure (pCO_2) was measured via triplicate 60-mL syringe headspace equilibrations (30-mL water/30-mL ambient air headspace, 5-min manual shake equilibration) directly injected into a PP Systems EGM-4 Infrared Gas Analyzer. Ambient air CO_2 concentration, water temperature, and equilibration temperature were measured for each equilibration in order to calculate pCO_2.

2.3. DIC, δ^{13}C-DIC, Δ^{14}C-DIC, and Keeling Incubations

Triplicate initial (t_0) and final (t_{28}) δ^{13}C-DIC analyses were undertaken from borosilicate glass serum vial headspaces after repressurization and equilibration with He gas on a Thermo Delta V Isotope Ratio Mass Spectrometer at Florida State University. Resulting $^{13}C/^{12}C$ ratios are reported in δ^{13}C notation relative to Vienna Pee Dee Belemnite. After samples had been run on the Isotope Ratio Mass Spectrometer, DIC was sparged as gaseous CO_2, trapped, distilled (i.e., cleaned of H_2O and other volatiles), quantified manometrically (Baratron, ±0.5 μM), and transferred into flame-sealed glass tubes. To procure enough C for radiocarbon analyses, the three replicates for t_0 and the three replicates for t_{28} were combined in the vacuum preparation line. DIC concentrations were calculated by dividing the combined mass by the aggregate volume of water in the three serum vials. Flame-sealed CO_2 samples were sent to the National Ocean Sciences Accelerator Mass Spectrometry Facility at the Woods Hole Oceanographic Institution for ^{14}C-DIC analyses, here reported in Δ^{14}C notation following Stuvier and Polach (1977).

The source and age of the DOC lost to bacterial biodegradation was estimated from the change in concentration and δ^{13}C and Δ^{14}C of the DIC pool over time using the Keeling plot method (Karlsson et al., 2007; Pataki et al., 2003). Briefly, the respiratory CO_2 produced in the water incubations adds to the background DIC already present, which increases the concentration of the DIC pool and changes its isotopic signature. As a result, a linear relationship exists between the δ^{13}C and Δ^{14}C isotopic signature and the inverse of DIC concentration (1/[DIC]), where the intercept of the relationship represents the isotopic composition of the respiratory CO_2, which we here relate to the sources and age of DOC along the fluvial network. Initial (t_0)

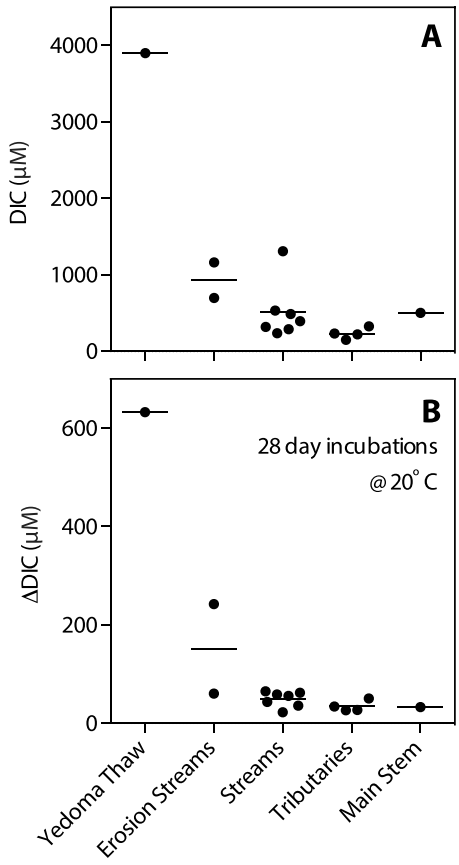

Figure 2. (a) Dissolved inorganic carbon concentrations and (b) change in dissolved inorganic carbon from sites spanning the fluvial network. The horizontal bars indicate average values for each site type. Change in dissolved inorganic carbon (ΔDIC) is the increase in DIC after 28-day incubations at 20 °C.

and final (t_{28}) isotopic ratios were averaged and plotted against their corresponding 1/[DIC] values and fitted with a linear regression. The *y*-intercept of the fitted line was determined to be the average isotopic signature of the DIC produced over the course of the 28-day bioincubation. To be clear, the *y*-intercepts reported are analytical solutions of two points (t_0 and t_{28}) rather than true linear regressions, since DIC concentrations were measured by combining the three replicates into one manometrically quantified sample and dividing by the total amount of sample water. To solve for the *y*-intercepts, initial (t_0) and final (t_{28}) triplicates were averaged for δ^{13}C-DIC, whereas the single, combined Δ^{14}C-DIC measurement was used for a given time point. To estimate a reasonable level of uncertainty, the standard deviation of the three δ^{13}C-DIC triplicates and the reported Δ^{14}C analytical error were propagated to the *y*-intercept solution.

2.4. DOC Concentration and DOM Composition

Dissolved organic carbon samples were thawed under refrigeration (4 °C), acidified with 12 N HCl to a pH of ~2, and measured via high-temperature catalytic oxidation on a Shimadzu TOC-LCPH analyzer. DOC concentrations are reported as the mean of at least three replicate injections for which the coefficient of variation was <2% (Mann et al., 2012). CDOM absorbance (*A*) was measured on a Horiba AquaLog Spectrophotometer. $SUVA_{254}$ values were calculated by dividing the decadic UV absorbance (*A*; m^{-1}) at λ = 254 nm by the DOC concentration (Weishaar et al., 2003).

Samples were prepared for Fourier transform ion cyclotron resonance mass spectrometry (FT-ICR MS) analysis by the solid-phase extraction of DOM method described in detail by Dittmar et al. (2008). Briefly, filtered samples were acidified to pH 2.3 with HPLC-grade HCl before solid phase extraction on 100-mg Bond Elut PPL (Agilent Technologies) cartridges. Sample volume was adjusted depending on original DOC concentration to obtain 40-μg C per mL of methanol eluate. Extracts were stored at −20 °C prior to being analyzed with a custom-built 9.4 Tesla FT-ICR MS equipped with a 22-cm diameter horizontal bore located at the National High Magnetic Field Laboratory (Tallahassee, Florida, USA; Blakney et al., 2011; Chen et al., 2014; Kaiser, Quinn, et al., 2011; Kaiser, Savory, et al., 2011; Kaiser et al., 2013). Negative ions were generated by means of direct infusion electrospray ionization at a flow rate of 500 nL min^{-1}, and 100 time domain acquisitions were coadded for each mass spectrum.

Molecular formulae were assigned (signals >6σ root mean square baseline noise) based on published rules (Koch et al., 2007; Stubbins et al., 2010) using an in-house designed software EnviroOrg ©™ (Corilo, 2015). Molecular formulas with elemental combinations of $C_{4\text{-}45}H_{8\text{-}92}N_{0\text{-}4}O_{1\text{-}25}S_{0\text{-}2}$ and mass errors less than 300 ppb were considered for assignment. Formulas were classified based on their elemental stoichiometries (Šantl-Temkiv et al., 2013). The modified aromaticity index (AI_{mod}) of each formula was calculated following the procedure of Koch and Dittmar (2006), and AI_{mod} values of 0.5 to 0.67 and >0.67 were classified as aromatic and condensed aromatic structures, respectively. Further compound classes were defined as follows using the script developed by Hemingway (2017): condensed aromatic = $AI_{mod} > 0.67$, polyphenolic = $0.67 \geq AI_{mod} > 0.5$, unsaturated low oxygen = $AI_{mod} < 0.5$, H/C < 1.5, O/C < 0.5; unsaturated high oxygen = $AI_{mod} < 0.5$, H/C < 1.5, O/C > 0.5; aliphatics = H/C 1.5–2.0, O/C < 0.9, N = 0; and peptides = H/C 1.5–2.0, O/C < 0.9, N > 0. It should be noted that assigning peptides can be ambiguous as they may also occur in alternative isomeric arrangements.

2.5. Correlation Statistics

All linear regressions, significance coefficients, and confidence intervals were determined with the statistical software Prism 6 by GraphPad. Mass spectrum Spearman rank correlation statistics were carried out by the Fourier transform Python package (Hemingway, 2017).

Table 1
Dissolved Inorganic Carbon (DIC) Concentration, Change in DIC After 28-Day Incubations (ΔDIC), CO_2 concentrations, and DIC Isotopes by Site Type

	n	DIC (μM)	ΔDIC (μM)	CO_2 (ppm)	Ambient δ^{13}C-DIC (‰)	Respiratory δ^{13}C-DIC (‰)	Ambient Δ^{14}C-DIC (‰)	Respiratory Δ^{14}C-DIC (‰)
Yedoma thaw	1	3,900	632	5,030	−11.8	−25.7	−713	−859
Erosion streams	2	933 ± 329	151 ± 91	667 ± 273	−10.6 ± 1.0	−26.0 ± 4.1	−329 ± 283	−374 ± 256
Streams	7	511 ± 368	49.1 ± 14.5	1,880 ± 521	−13.5 ± 2.3	−24.1 ± 2.2	−29.0 ± 49.0	−2.44 ± 58.5
Tributaries	4	235 ± 72.2	34.6 ± 9.6	618 ± 209	−7.67 ± 2.3	−19.6 ± 1.9	−95.0 ± 23.6	−27.0 ± 34.0
Main stem	1	503	33	606	−7.58	−17.4	−131	−71

Note. Data are reported as averages ± standard deviation for each site type.

3. Results

3.1. DIC, ΔDIC, and CO_2

Ambient DIC concentrations ranged from 153 to 3,903 μM and were generally higher in streams compared to tributaries and the Kolyma main stem (Figure 2a and Table 1). Change in DIC over 28-day bioincubations (ΔDIC or DIC produced) ranged from 22.7 to 632 μM and reflected a similar trend as ambient concentrations through the fluvial network, with samples from permafrost-dominated streams and small streams producing more DIC than larger rivers (Figure 2b and Table 1). Dissolved CO_2 concentrations ranged from 412 to 5,030 ppm and followed a similar pattern as DIC concentrations, generally decreasing moving down the watershed toward the main stem (Table 1).

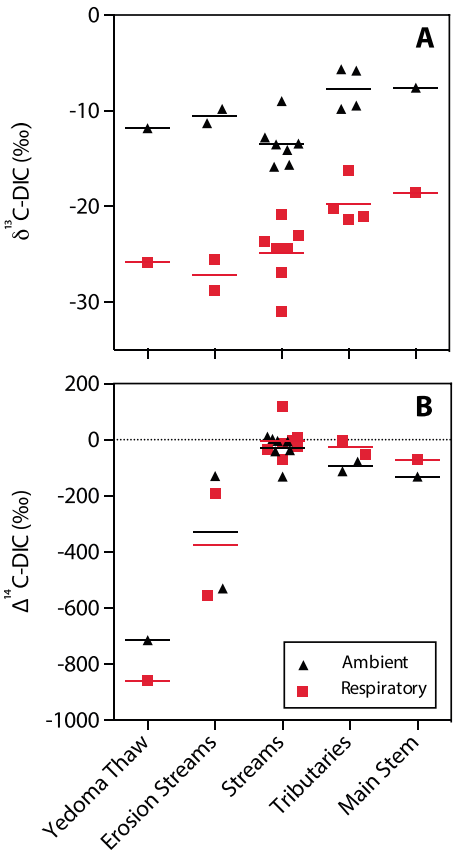

Figure 3. (a) δ^{13}C and (b) Δ^{14}C of ambient and respiratory dissolved inorganic carbon from sites spanning the fluvial network. The black triangles represent ambient values. The red squares represent respiratory values derived from 28-day keeling plot incubations. The horizontal bars indicate average values for a given site type.

3.2. Ambient and Respiratory δ^{13}C-DIC and Δ^{14}C-DIC

Ambient δ^{13}C-DIC ranged from −15.9 to −5.8‰ and was most depleted and exhibited greatest variability in low-order streams (Figure 3a and Table 1). Larger tributaries and the Kolyma River main stem exhibited more enriched δ^{13}C-DIC values relative to low-order streams (Figure 3a). Respiratory δ^{13}C-DIC values derived from Keeling plots ranged from −28.8 to −16.3‰ and also generally became enriched in higher-order fluvial sites (Figure 3a and Table 1). Streams, including erosion streams, exhibited the widest range of respiratory δ^{13}C-DIC values. Respiratory δ^{13}C-DIC values were universally depleted relative to ambient values. Respiratory δ^{13}C-DIC produced in permafrost streams and streams was generally more depleted than DIC produced in larger tributaries or the main stem of the Kolyma River. Offsets between respiratory and ambient δ^{13}C-DIC ranged from 7.4 to 17.5‰ with an average value of 11.8‰ and with no clear pattern across the fluvial network (Figure S1a in the supporting information).

Ambient Δ^{14}C-DIC values ranged from −713 to 11‰ and were generally near modern in radiocarbon age (i.e., more ^{14}C enriched; modern defined as Δ^{14}C = 0‰) except for the Yedoma thaw stream and one of the erosion streams (Figure 3b and Table 1). Aside from the aged signature observed in the permafrost-dominated streams, ambient Δ^{14}C-DIC became slightly depleted (older) moving from streams to tributaries and the Kolyma River main stem. Respiratory Δ^{14}C-DIC values ranged from −859 to +117‰ and generally tracked their ambient counterparts. Respiratory Δ^{14}C-DIC was predominantly near modern throughout the fluvial network, except for the Yedoma thaw stream and the two erosion streams (Figure 3b and Table 1). Offsets between respiratory and ambient Δ^{14}C-DIC ranged from −108 to +145‰ (Figure S2b). In permafrost-dominated streams, respiratory Δ^{14}C-DIC was more depleted (older) than ambient. Relative to ambient, respiratory Δ^{14}C-DIC in streams ranged from both depleted (older) to

Table 2
Dissolved Organic Carbon (DOC) Concentration, Specific UV Absorbance at 254 nm ($SUVA_{254}$), and DOM Composition by Fourier Transform Ion Cyclotron Resonance Mass Spectrometry by Site Type

	n	Initial DOC (μM)	$SUVA_{254}$ (l mg C^{-1} m^{-1})	Assigned formulae	CHO (# of formulae)	CHON (# of formulae)	Condensed aromatics	Polyphenols	Unsaturated low oxygen	Unsaturated high oxygen	Aliphatics	Peptides
Yedoma thaw	1	1,2492	1.4	8,353	4,350 (52.1%)	3,043 (36.4%)	343 (4.1%)	1,052 (12.6%)	2,414 (28.9%)	3,212 (38.5%)	1,023 (12.2%)	309 (3.7%)
Erosion streams	2	2,157 ± 903	2.56 ± .14	8,992 ± 813	5,630 ± 14 (62.6%)	2,603 ± 1,037 (28.9%)	623 ± 113 (6.9%)	1,559 ± 184 (17.3%)	2,526 ± 188 (28.1%)	3,494 ± 114 (39.1%)	702 ± 168 (7.7%)	89 ± 48 (0.9%)
Streams	7	1,667 ± 167	3.18 ± .12	8,228 ± 305	5,451 ± 339 (66.3%)	2,076 ± 425 (25.2%)	530 ± 49 (6.4%)	1,430 ± 86 (17.3%)	2,243 ± 86 (27.3%)	3,495 ± 111 (42.6%)	457 ± 22 (5.6%)	71 ± 18 (0.9%)
Tributaries	4	523 ± 49	2.91 ± .13	8,224 ± 384	5,263 ± 302 (64.0%)	2,133 ± 614 (25.9%)	491 ± 38 (5.9%)	1,416 ± 66 (17.2%)	2,357 ± 105 (28.7%)	3,337 ± 122 (40.7%)	565 ± 53 (6.8%)	57 ± 8 (0.7%)
Main stem	1	327	2.88	7,587	5,268 (69.4%)	1,620 (21.4%)	425 (5.6%)	1,255 (16.5%)	2,313 (30.5%)	3,026 (39.9%)	533 (7.0%)	35 (0.5%)

Note. Composition data are reported in average number of assigned formulae ± standard deviation for each compound subclass. Average percent of total compounds for each subclass are reported in parentheses.

enriched (younger). In tributaries and the main stem of the Kolyma, respiratory Δ^{14}C-DIC was enriched (younger) relative to ambient. Overall, offsets between respiratory and ambient Δ^{14}C-DIC became progressively more positive (enriched) moving from permafrost-dominated streams through the fluvial network to the Kolyma River main stem (Figure S2b).

3.3. DOC and FT-ICR MS

Dissolved organic carbon concentrations ranged from 327 to 12,492 μM and followed a similar decreasing trend as DIC concentrations through the fluvial network (Table 2). Permafrost-dominated streams exhibited the highest concentrations followed by small streams, tributaries, and the Kolyma River main stem. $SUVA_{254}$ ranged from 1.40 to 3.18 L mg C^{-1} m^{-1} and was lowest in permafrost-dominated streams (Table 1). Small streams generally exhibited higher $SUVA_{254}$ values than larger tributaries or the Kolyma River main stem (Table 1).

Dissolved organic matter composition by FT-ICR MS revealed between 6,477 and 9,805 assigned molecular formulae (Table 2). Erosion streams displayed the highest average number of assigned formulae (8,992), followed by the Yedoma thaw (8,535), streams (8,228), tributaries (8,224), and the main stem (7,587). For all sites, unsaturated low- and high-oxygen compound classes predominated, making up 67.4 to 71.7% of all the total assigned formulae (Table 2). Except for the Yedoma thaw site, average number of condensed aromatic and polyphenolic compounds decreased downstream through the fluvial network, starting with erosion streams (623 and 1,559, respectively) and moving to streams (530, 1,430), tributaries (491, 1,416), and ultimately the main stem (425, 1,255; Table 2). The Yedoma thaw site had relatively low contributions of condensed aromatics and polyphenolics (343 and 1,052, respectively). The highest average number of aliphatic and peptide compounds were found in the Yedoma thaw (1,023 and 309, respectively) and amounted to 12.2 and 3.7% of total assigned formulae, respectively. Apart from the low average aliphatic compound contributions in streams, aliphatic and peptide compounds decreased through the fluvial network from erosion streams (702 and 89, respectively), to streams (457, 71), tributaries (565, 57), and the main stem (533, 35), comprising between 5.6–7.7% (for aliphatics) and 0.5–0.9% (for peptides) of total assigned formulae (Table 2).

4. Discussion

4.1. Fueling Microbial Respiration in an Arctic Fluvial Network

Respiratory δ^{13}C and Δ^{14}C-DIC signatures showed a shifting source of substrate for microbial respiration through the fluvial network (Figure 4). In the Yedoma thaw stream, microbes respired predominantly aged, permafrost-derived OC (Δ^{14}C-depleted). In the erosion streams, the respiratory signature was a mixture of aged permafrost and modern terrestrial carbon. A definitive signature of respiratory or ambient aged DIC was not detected in any of the other streams, tributaries, or the main stem of the Kolyma River. Moving downstream from headwater streams to the main stem, respiratory δ^{13}C-DIC became more enriched (Figure 3a), suggesting that microbial respiration shifted from modern allochthonous terrestrial carbon to modern autochthonous aquatic biomass sources. Generally, these results provide an independent corroboration of the results from Mann et al. (2015), which used ^{14}C-DOC consumption as a tracer instead of ^{14}C-DIC production and found a similar downstream shift from permafrost to modern allochthonous and autochthonous DOM substrates for respiration.

There are two potentially complementary explanations for why respiratory and ambient permafrost DIC signatures were not found throughout the Kolyma fluvial network. First, the quantity of thawed and mobilized DOC from permafrost soils could be small relative to the modern plant-derived C pool. Our sites were sampled at the time of the deepest active-layer thaw (late August/early September), when permafrost DOC mobilization to streams would have been near its annual maximum, especially relative to modern plant-derived C, which is predominantly transported during the spring freshet (Mann et al., 2012; Spencer et al., 2008). The second explanation is that permafrost OC is highly biolable and is rapidly respired upon thaw before fluvial transport can occur (Panneer Selvam et al., 2017), particularly transport to the mouth of a major Arctic River like the

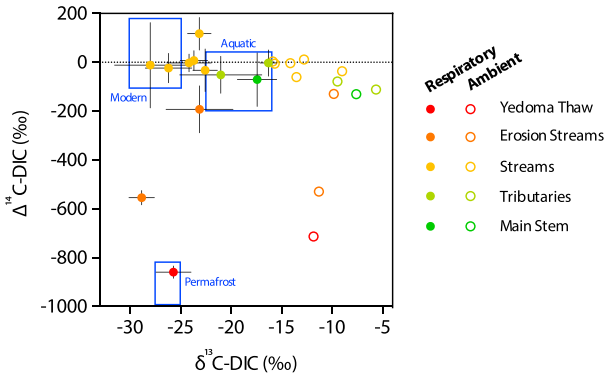

Figure 4. Distribution of δ^{13}C-dissolved inorganic carbon (DIC) and Δ^{14}C-DIC isotopes across the fluvial network. Site type is indicated by color (red to green). Ambient values are shown as open circles. Error ranges for ambient values do not exceed the symbol size. Respiratory values are shown as filled circles with error bars. Isotopic ranges of permafrost, modern, and aquatic carbon sources are shown in blue boxes following Mann et al. (2015).

Kolyma. Indeed, multiple experimental studies have demonstrated such high biolability for Yedoma thaw DOC (Drake et al., 2015; Mann et al., 2015; Vonk et al., 2013).

This high biolability could explain the absence of an aged respiratory DIC signature in the bioincubations from downstream samples (since it would have all been consumed before sampling), but it is an open question as to whether pore water or upstream respiration would impart a detectable aged signature on the ambient DIC pool. We hypothesized that it would, given its high biolability relative to modern vegetation (Spencer et al., 2015). Yet we acknowledge that the total amount of respiratory CO_2 derived from permafrost OC is the ultimate factor that would change the ambient Δ^{14}C-DIC signature, and not the rate of permafrost OC consumption or its relative biolability, per se. If additions of respiratory CO_2 from permafrost were sufficiently small relative to any other source of DIC, it would easily be masked. For example, if respiration of ancient permafrost-derived OC (Δ^{14}C of −1,000‰; i.e., radiocarbon dead minimum value) represented 10% of total aquatic respiration and respiration of modern OC (Δ^{14}C of 0‰) comprised the remaining 90%, the resultant DIC would have an Δ^{14}C signature of −100‰, which is within the bounds of a modern vegetation end-member for the Kolyma Basin (Mann et al., 2015). In this example, a 10% subsidy of total respiration by permafrost-derived OC would still represent a substantial contribution, indicative of high rates of thaw and mobilization (Schuur et al., 2015; Vonk & Gustafsson, 2013).

In addition to the masking of permafrost-sourced CO_2 by respiration of modern OC, CO_2 lost via outgassing may have simply removed aged DIC from the system. In most fluvial networks, headwater streams exhibit the highest CO_2 outgassing given their high gas concentrations, high surface area to volume ratios, and higher turbulence relative to downstream tributaries and rivers (Butman & Raymond, 2011). If the same patterns extend to the Kolyma fluvial network, faster physical loss of CO_2 would coincide with the regions of the fluvial network that have the highest potential to contain permafrost-sourced CO_2 (given permafrost DOM's high biolability upon thaw) and thus proportionately remove the respiration signature of permafrost relative to modern vegetation. Furthermore, inputs of bicarbonate (HCO_3^-) from chemical weathering of silicate or carbonate minerals could also lower bulk ambient Δ^{14}C-DIC, depending on the source of CO_2 involved in the reaction and the proportion of carbonate weathering. However, permafrost has been shown to decrease the export of major ions like HCO_3^- by limiting the interaction between surface waters and bedrock while simultaneously preventing mineral-rich groundwater from reaching the surface (Frey & McClelland, 2009). Regardless, the inputs of aged DIC from either permafrost or carbonate weather are assumed to be low relative to those from the respiration of modern DIC, given that the ambient Δ^{14}C-DIC values were all near the modern range for the Kolyma (Figure 3b). In short, masking by modern respiration in concert with high rates of CO_2 loss from headwater reaches of the fluvial network may explain why aged DIC was not detected outside of a few sites dominated by thaw from permafrost soils.

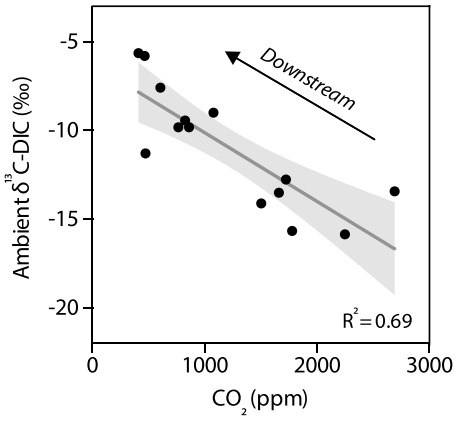

Figure 5. Ambient δ^{13}C-DIC as a function of CO_2 concentration. The solid gray line is the linear regression (ambient δ^{13}C-dissolved inorganic carbon = −0.00387 * CO_2 − 6.25; R^2 = 0.69), and the shaded light gray bands are the 95% confidence intervals. The "downstream" arrow indicates the general pattern of decreasing CO_2 concentration moving from low to high-order streams observed across the fluvial network.

Despite the slight difference in δ^{13}C-DOC values between permafrost (−26.3 ± 1.3‰) and contemporary vegetation (−28.5 ± 2.0‰; Mann et al., 2015), respiratory δ^{13}C-DIC results from this study did not allow for the identification of permafrost OC sources. This is because all of the respiratory δ^{13}C-DIC values in this study lied within the modern vegetation and aquatic autochthonous end-member ranges (Figure 4). Ambient δ^{13}C-DIC values from this study (−15.9 to −7.6‰) compared well to values reported from other Arctic watersheds in Alaska (approx. −20 to −8‰; Throckmorton et al., 2015).

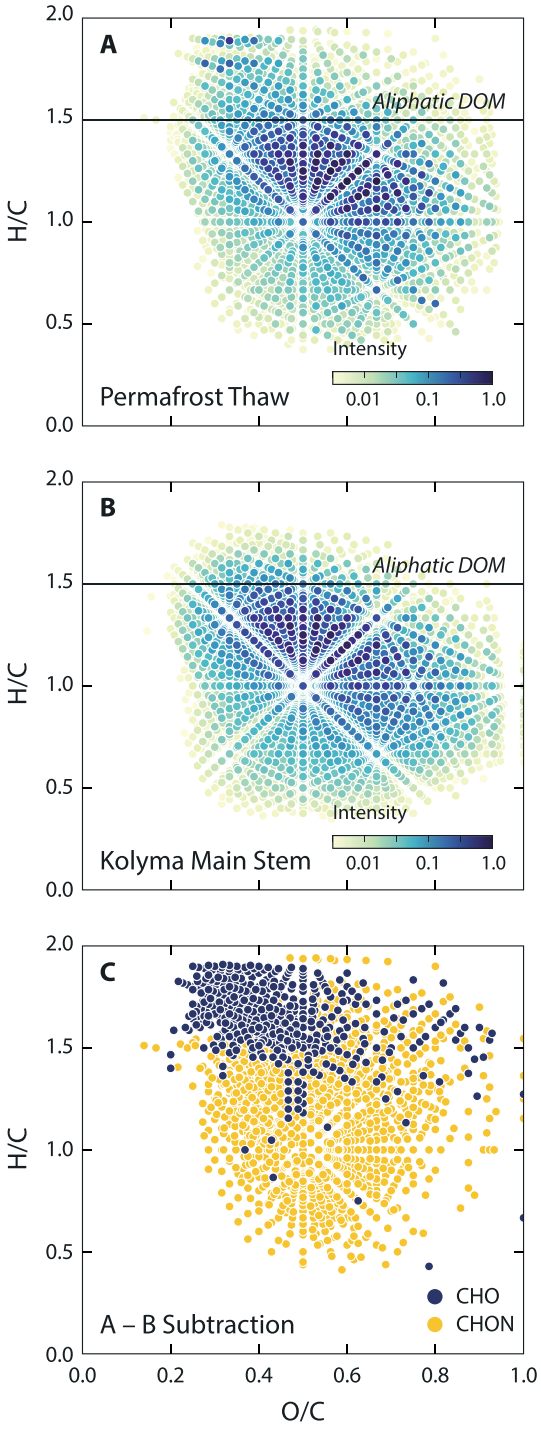

Figure 6. Van Krevelen plots of initial dissolved organic carbon from (a) Yedoma thaw and the (b) Kolyma River main stem. The yellow to blue color gradient represents the relative normalized intensity of each molecular formula ranging from 0 to 1. (a) and (b) are both scaled to the most intense peak found in either sample. (c) Unique formulae present in the Yedoma thaw relative to the Kolyma River main stem, differentiated by nitrogen free (blue) and N-containing (orange) compounds.

Results from this study show that ambient δ^{13}C-DIC was universally enriched relative to respiratory δ^{13}C-DIC (Figure 3a). This suggests that either the initial pore or rainwater DIC was enriched or it started as the depleted product of soil respiration and became fractionated during downstream transport (Campeau et al., 2017). We suggest that CO_2 off-gassing may have fractionated the DIC pool, since DIC concentrations significantly decreased downstream (Figure 2a), while ambient δ^{13}C-DIC became more enriched (Figure 5). Off-gassing of CO_2 has been shown to strongly enrich the ambient δ^{13}C-DIC pool over short distances downstream, since equilibrium fractionation of the carbonate system preferentially leaves ^{12}C in the CO_2 phase, which is the only phase available for off-gassing (Doctor et al., 2008). Off-gassing would also potentially explain why there was no downstream aged signature in the ambient DIC pool (discussed in the ^{14}C section above). We acknowledge that downstream δ^{13}C enrichment could have resulted from other processes such as photosynthesis or weathering inputs, but we suggest that it is unlikely due to (a) the strong downstream enrichment trend accompanied by a loss in DIC which is consistent with off-gassing, (b) limitations on light availability posed by high turbidity and colored DOM present in the Kolyma watershed, and (c) the limited interaction between surface waters and minerals due to permafrost. Regardless, this masking of the ambient δ^{13}C-DIC illustrates the difficulty of using this tracer to determine DIC sources (Campeau et al., 2017; Giesler et al., 2013).

4.2. Linking DOM Composition to Respiratory DIC

Fourier transform ion cyclotron resonance mass spectrometry compositional analysis of DOM revealed proportionately high aliphatic and high N-containing compounds in the permafrost-dominated streams compared to the rest of the fluvial network (Table 2 and Figure 6). DOM from the Yedoma thaw site (the most permafrost influenced site) was both absolutely and proportionately higher in aliphatics and peptides while proportionately lower in polyphenols relative to other sites (Table 2). In addition to the unique proportions of molecular formulae, the Yedoma thaw site exhibited high relative abundances throughout the compound classes compared to the Kolyma River (Figure 6a). These results are consistent with other DOM compositional studies that found that permafrost thaw had a unique molecular signature compared to Arctic surface waters due to its high aliphatic content (Spencer et al., 2015) and that DOM leached from permafrost soils was relatively enriched in low-molecular weight, saturated, and less-oxidized compounds (Ward & Cory, 2015). When comparing the thousands of molecular formulae reported in DOM from the Yedoma thaw site (Figure 6a) with those found in the Kolyma River (Figure 6b), a number of molecular formulae with relatively high H/C CHO and lower H/C N-containing compounds were found to be uniquely present in the permafrost site (Figure 6c). These compounds are generally energy-rich and biolabile due to their high H/C ratios and amine content (Hopkinson et al., 1998; Rossel et al., 2013; Spencer et al., 2015). Accordingly, it has been demonstrated that these metabolically favorable compounds are preferentially consumed by microbes over short timeframes (Berggren et al., 2010; Drake et al., 2015; O'Donnell et al., 2016; Spencer et al., 2015; Ward & Cory, 2015).

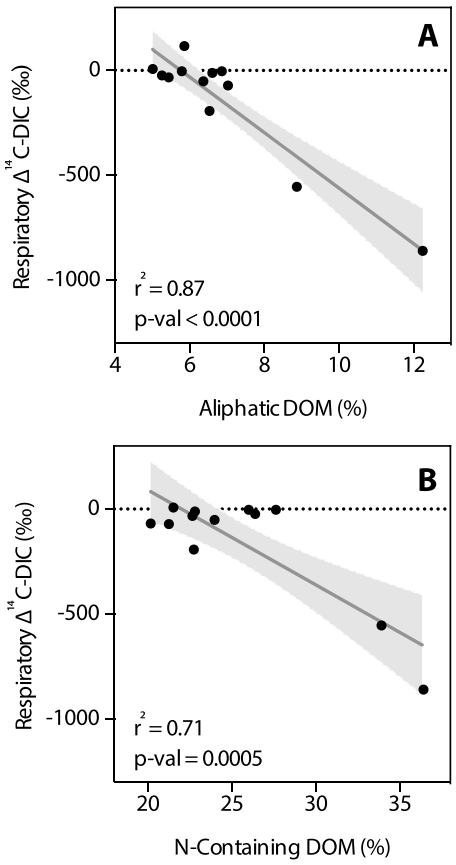

Figure 7. Respiratory Δ^{14}C-dissolved inorganic carbon as a function of the percent of (a) aliphatic and (b) N-containing compounds in the initial dissolved organic carbon. The solid gray lines are the linear regressions, and the shaded light gray bands are the 95% confidence intervals.

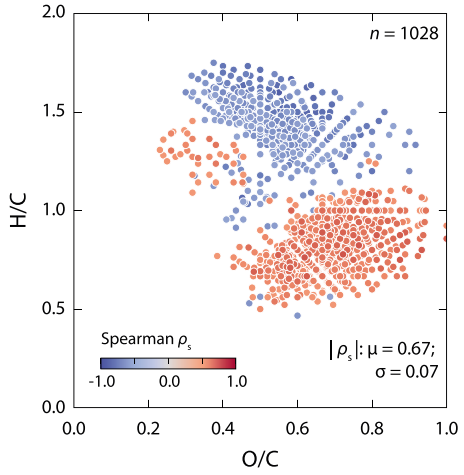

Figure 8. Van Krevelen plots of the Spearman rank correlation coefficients (ρ_S) between relative intensity and respiratory Δ^{14}C-dissolved inorganic carbon (DIC) for molecular formulae present in all samples throughout the fluvial network. Only formulae that exhibit a statistically significant correlation with Δ^{14}C-DIC are shown (P value ≤ 0.05, $n = 1{,}028$). Formulae with negative ρ_S values (blue) exhibit higher intensities in samples with lower respiratory Δ^{14}C-DIC values, while formulae with positive ρ_S values (red) exhibit the opposite. The mean of the absolute value of ρ_S for all plotted formulae was 0.67, and the standard deviation was 0.07.

In our study, high initial % aliphatic and initial % N-containing DOM content were significantly correlated with an aged radiocarbon signature of respiratory DIC, suggesting that these highly biolabile compounds are sourced from permafrost and respired by microbes as aged CO_2 throughout the fluvial network (Figures 7a and 7b). Furthermore, on examination of the 4,670 molecular formulae shared by all sites, the relative intensities of 1,028 were found to be significantly correlated (P value < 0.05) with respiratory Δ^{14}C-DIC (Figure 8). Among these significantly correlated compounds, a clear divide between aliphatic, high H/C DOM (positively correlated with more depleted respiratory Δ^{14}C-DIC) and more aromatic, low H/C DOM (positively correlated with more enriched respiratory Δ^{14}C-DIC) emerged (Figure 8). This analysis clearly adds further support to the assertion that when bacteria respires aged OC, such as permafrost DOM, it is being predominantly sourced from aliphatic DOM. Conversely, when bacteria respires more modern sources of OC, it is associated with more aromatic, less-saturated DOM typical of plant-derived material (Ward et al., 2013). Overall, this correlation suggests that the compositional distinction between permafrost and modern terrestrial DOM drives the production of aged versus modern CO_2, respectively. Moreover, these findings add support to the second explanation for a lack of permafrost signatures throughout the fluvial network, which is that these highly biolabile compounds unique to permafrost are simply respired before downstream transport can occur.

The results from this study exemplify the difficulties of sensitively assessing permafrost mobilization using currently available geochemical tracers at the watershed scale. The aliphatic and N-containing compounds unique to permafrost (Figure 6) have been shown to be readily bioavailable and so do not persist long after thaw in fluvial ecosystems (Spencer et al., 2015; Ward & Cory, 2015). With respect to the remainder of the molecular formulae identified via FT-ICR MS, the majority are not unique to permafrost and have been reported in other studies (Kellerman et al., 2014; O'Donnell et al., 2016; Stubbins et al., 2010). Compared to the unique molecular formulae found in permafrost, the compounds produced during bioincubation of permafrost DOM and the remnant stable compounds are lower in H/C and N-containing formulae. From a molecular standpoint, these compounds are highly comparable to those produced by modern vegetation (and their corresponding degradation products), which are found throughout major Arctic rivers (Medeiros et al., 2016; Spencer et al., 2015). The inorganic by-products of permafrost respiration, identified by their aged radiocarbon signatures in the DIC pool, are also not ideal tracers in the real world since their depleted Δ^{14}C values are proportionately overwhelmed by the signature of modern C. However, results from this study show that when there is massive thaw or proportionately high inputs from permafrost soils relative to modern surface soils, an aged signature can be detected in the DIC pool.

4.3. Fate of Aged OC in Fluvial Networks

Overall, the findings from this study suggest that substrate availability determines the source of carbon respired by microbes in Arctic streams and rivers. In the Kolyma fluvial network, C isotopes in respiratory DIC reveal a downstream OC biolability continuum, starting with permafrost-derived OC, transitioning to modern terrestrial C, and

then ultimately aquatic biomass. Given the chemical composition of permafrost OC (high H/C ratio and high N-containing formulae), it is highly biolabile and therefore does not persist within the fluvial network. The by-product of permafrost OC biodegradation, aged DIC, is only found where there is a high initial proportion of aged OC, since its isotopic signature is both overprinted by physical processes and overwhelmed by DIC produced during the respiration of modern OC. The loss of aged DOC to microbial respiration and the masking of aged DIC by both modern DIC and fractionation processes confound efforts to quantify the amount and fate of permafrost mobilized to fluvial networks.

Importantly, the observed high biolability of aged OC and the downstream lability-age continuum may apply to systems outside of the Arctic, provided these systems receive aged components of varying composition in unknown proportion to modern organic matter (Barnes et al., 2018; Guillemette et al., 2017). In such circumstances where the loss of aged carbon is masked by modern processes, the methods described in this study may assist in connecting the age of DOM with the processes by which it is biologically and physically fractionated from soils to fluvial networks (Hutchins et al., 2017). Ultimately, the integration and layering of these DOM and DIC age dynamics into frameworks like the "River Continuum Concept" or the "River as a Chemostat" will help biogeochemists better partition the cycling of modern versus aged carbon and propel research in this important domain (Creed et al., 2015; Vannote et al., 1980).

Acknowledgments
We thank the staff at the Northeast Science Station in Chersky for their assistance with field sampling. This work was funded by NSF grants ANT-1203885 and PLR-1500169 to R.G.M.S. Work partially supported by NSF (DMR-1157490), State of Florida, and the FSU Future Fuels Institute. The authors thank all people in the NHMFL ICR Program that work to facilitate data acquisition and processing for users of the facility. We also thank Greg Fiske at the Woods Hole Research Center for making the site map. F.G. was partly supported by a postdoctoral fellowship from the Fond de Recherche du Québec—Nature et Technologies. All data presented in the figures and summarized in the tables can be found in the Supplementary Excel file online.

References

Abbott, B. W., Larouche, J. R., Jones, J. B., Bowden, W. B., & Balser, A. W. (2014). Elevated dissolved organic carbon biodegradability from thawing and collapsing permafrost. *Journal of Geophysical Research: Biogeosciences*, *119*, 2049–2063. https://doi.org/10.1002/2014JG002678

Barnes, R. T., Butman, D. E., Wilson, H. F., & Raymond, P. A. (2018). Riverine export of aged carbon driven by flow path depth and residence time. *Environmental Science & Technology*. https://doi.org/10.1021/acs.est.7b04717

Berggren, M., Laudon, H., Haei, M., Ström, L., & Jansson, M. (2010). Efficient aquatic bacterial metabolism of dissolved low-molecular-weight compounds from terrestrial sources. *The ISME Journal*, *4*(3), 408–416. https://doi.org/10.1038/ismej.2009.120

Blakney, G. T., Hendrickson, C. L., & Marshall, A. G. (2011). Predator data station: A fast data acquisition system for advanced FT-ICR MS experiments. *International Journal of Mass Spectrometry*, *306*(2-3), 246–252. https://doi.org/10.1016/j.ijms.2011.03.009

Butman, D., & Raymond, P. A. (2011). Significant efflux of carbon dioxide from streams and rivers in the United States. *Nature Geoscience*, *4*(12), 839–842. https://doi.org/10.1038/ngeo1294

Campeau, A., Wallin, M. B., Giesler, R., Löfgren, S., Mörth, C.-M., Schiff, S., et al. (2017). Multiple sources and sinks of dissolved inorganic carbon across Swedish streams, refocusing the lens of stable C isotopes. *Scientific Reports*, *7*(1), 9158.

Chen, T., Beu, S. C., Kaiser, N. K., & Hendrickson, C. L. (2014). Note: Optimized circuit for excitation and detection with one pair of electrodes for improved Fourier transform ion cyclotron resonance mass spectrometry. *The Review of Scientific Instruments*, *85*(6), 066107.

Corilo, Y. (2015). *EnviroOrg*. Tallahassee, FL: Florida State University.

Creed, I. F., McKnight, D. M., Pellerin, B. A., Green, M. B., Bergamaschi, B. A., Aiken, G. R., et al. (2015). The river as a chemostat: Fresh perspectives on dissolved organic matter flowing down the river continuum. *Canadian Journal of Fisheries and Aquatic Sciences. Journal Canadien Des Sciences Halieutiques et Aquatiques*, *72*(8), 1272–1285.

Dittmar, T., Koch, B. P., Hertkorn, N., & Kattner, G. (2008). A simple and efficient method for the solid-phase extraction of dissolved organic matter (SPE-DOM) from seawater. *Limnology and Oceanography, Methods / ASLO*, 6(6), 230–235. https://doi.org/10.4319/lom.2008.6.230

Doctor, D. H., Kendall, C., Sebestyen, S. D., Shanley, J. B., Ohte, N., & Boyer, E. W. (2008). Carbon isotope fractionation of dissolved inorganic carbon (DIC) due to outgassing of carbon dioxide from a headwater stream. *Hydrological Processes*, *22*(14), 2410–2423. https://doi.org/10.1002/hyp.6833

Drake, T. W., Wickland, K. P., Spencer, R. G. M., McKnight, D. M., & Striegl, R. G. (2015). Ancient low–molecular-weight organic acids in permafrost fuel rapid carbon dioxide production upon thaw. *Proceedings of the National Academy of Sciences of the United States of America*, *112*(45), 13,946–13,951. https://doi.org/10.1073/pnas.1511705112

Frey, K. E., & McClelland, J. W. (2009). Impacts of permafrost degradation on arctic river biogeochemistry. *Hydrological Processes*, *23*(1), 169–182. https://doi.org/10.1002/hyp.7196

Giesler, R., Mörth, C.-M., Karlsson, J., Lundin, E. J., Lyon, S. W., & Humborg, C. (2013). Spatiotemporal variations of pCO2 and δ13C-DIC in subarctic streams in northern Sweden. *Global Biogeochemical Cycles*, *27*, 176–186. https://doi.org/10.1002/gbc.20024

Guillemette, F., Bianchi, T. S., & Spencer, R. G. M. (2017). Old before your time: Ancient carbon incorporation in contemporary aquatic food webs. *Limnology and Oceanography*, *62*(4), 1682–1700. https://doi.org/10.1002/lno.10525

Guo, L., Ping, C.-L., & Macdonald, R. W. (2007). Mobilization pathways of organic carbon from permafrost to arctic rivers in a changing climate. *Geophysical Research Letters*, *34*, L13603. https://doi.org/10.1029/2007GL030689

Hemingway, J. (2017). Fourier transform: Open-source tools for FT-ICR MS data analysis. Retrieved from http://github.com/FluvialSeds/fouriertransform [online]

Hopkinson, C. S., Buffam, I., Hobbie, J., Vallino, J., Perdue, M., Eversmeyer, B., et al. (1998). Terrestrial inputs of organic matter to coastal ecosystems: An intercomparison of chemical characteristics and bioavailability. *Biogeochemistry*, *43*(3), 211–234. https://doi.org/10.1023/A:1006016030299

Hutchins, R. H. S., Aukes, P., Schiff, S. L., Dittmar, T., Prairie, Y. T., & Giorgio, P. A. (2017). The optical, chemical, and molecular dissolved organic matter succession along a boreal soil-stream-river continuum. *Journal of Geophysical Research: Biogeosciences*, *122*, 2892–2908. https://doi.org/10.1002/2017JG004094

Kaiser, N. K., McKenna, A. M., Savory, J. J., Hendrickson, C. L., & Marshall, A. G. (2013). Tailored ion radius distribution for increased dynamic range in FT-ICR mass analysis of complex mixtures. *Analytical Chemistry*, *85*(1), 265–272. https://doi.org/10.1021/ac302678v

Kaiser, N. K., Quinn, J. P., Blakney, G. T., Hendrickson, C. L., & Marshall, A. G. (2011). A novel 9.4 Tesla FTICR mass spectrometer with improved sensitivity, mass resolution, and mass range. *Journal of the American Society for Mass Spectrometry*, *22*(8), 1343–1351. https://doi.org/10.1007/s13361-011-0141-9

Kaiser, N. K., Savory, J. J., McKenna, A. M., Quinn, J. P., Hendrickson, C. L., & Marshall, A. G. (2011). Electrically compensated Fourier transform ion cyclotron resonance cell for complex mixture mass analysis. *Analytical Chemistry*, *83*(17), 6907–6910. https://doi.org/10.1021/ac201546d

Karlsson, J., Jansson, M., & Jonsson, A. (2007). Respiration of allochthonous organic carbon in unproductive forest lakes determined by the Keeling plot method. *Limnology and Oceanography*, *52*(2), 603–608. https://doi.org/10.4319/lo.2007.52.2.0603

Kellerman, A. M., Dittmar, T., Kothawala, D. N., & Tranvik, L. J. (2014). Chemodiversity of dissolved organic matter in lakes driven by climate and hydrology. *Nature Communications*, *5*, 3804.

Koch, B. P., & Dittmar, T. (2006). From mass to structure: An aromaticity index for high-resolution mass data of natural organic matter. *Rapid Communications in Mass Spectrometry: RCM*, *20*(5), 926–932. https://doi.org/10.1002/rcm.2386

Koch, B. P., Dittmar, T., Witt, M., & Kattner, G. (2007). Fundamentals of molecular formula assignment to ultrahigh resolution mass data of natural organic matter. *Analytical Chemistry*, *79*(4), 1758–1763. https://doi.org/10.1021/ac061949s

Mann, P. J., Davydova, A., Zimov, N., Spencer, R. G. M., Davydov, S., Bulygina, E., et al. (2012). Controls on the composition and lability of dissolved organic matter in Siberia's Kolyma River basin. *Journal of Geophysical Research*, *117*, G01028. https://doi.org/10.1029/2011JG001798

Mann, P. J., Eglinton, T. I., McIntyre, C. P., Zimov, N., Davydova, A., Vonk, J. E., et al. (2015). Utilization of ancient permafrost carbon in headwaters of Arctic fluvial networks. *Nature Communications*, *6*(1), 7856. https://doi.org/10.1038/ncomms8856

Medeiros, P. M., Seidel, M., Niggemann, J., Spencer, R. G. M., Hernes, P. J., Yager, P. L., et al. (2016). A novel molecular approach for tracing terrigenous dissolved organic matter into the deep ocean. *Global Biogeochemical Cycles*, *30*, 689–699. https://doi.org/10.1002/2015GB005320

Neff, J. C., Finlay, J. C., Zimov, S. A., Davydov, S. P., Carrasco, J. J., Schuur, E. A. G., & Davydova, A. I. (2006). Seasonal changes in the age and structure of dissolved organic carbon in Siberian rivers and streams. *Geophysical Research Letters*, *33*, L23401. https://doi.org/10.1029/2006GL028222

O'Donnell, J. A., Aiken, G. R., Butler, K. D., Guillemette, F., Podgorski, D. C., & Spencer, R. G. M. (2016). DOM composition and transformation in boreal forest soils: The effects of temperature and organic-horizon decomposition state. *Journal of Geophysical Research: Biogeosciences*, *121*, 2727–2744. https://doi.org/10.1002/2016JG003431

Panneer Selvam, B., Lapierre, J.-F., Guillemette, F., Voigt, C., Lamprecht, R. E., Biasi, C., et al. (2017). Degradation potentials of dissolved organic carbon (DOC) from thawed permafrost peat. *Scientific Reports*, *7*, 45811. https://doi.org/10.1038/srep45811

Pataki, D. E., Ehleringer, J. R., Flanagan, L. B., Yakir, D., Bowling, D. R., Still, C. J., et al. (2003). The application and interpretation of Keeling plots in terrestrial carbon cycle research. *Global Biogeochemical Cycles*, *17*(1), 1022. https://doi.org/10.1029/2001GB001850

Raymond, P. A., McClelland, J. W., Holmes, R. M., Zhulidov, A. V., Mull, K., Peterson, B. J., et al. (2007). Flux and age of dissolved organic carbon exported to the Arctic Ocean: A carbon isotopic study of the five largest arctic rivers. *Global Biogeochemical Cycles*, *21*, GB4011. https://doi.org/10.1029/2007GB002934

Rossel, P. E., Vähätalo, A. V., Witt, M., & Dittmar, T. (2013). Molecular composition of dissolved organic matter from a wetland plant (Juncus effusus) after photochemical and microbial decomposition (1.25 yr): Common features with deep sea dissolved organic matter. *Organic Geochemistry*, *60*, 62–71. https://doi.org/10.1016/j.orggeochem.2013.04.013

Šantl-Temkiv, T., Finster, K., Dittmar, T., Hansen, B. M., Thyrhaug, R., Nielsen, N. W., & Karlson, U. G. (2013). Hailstones: A window into the microbial and chemical inventory of a storm cloud. *PLoS One*, *8*(1), e53550.

Schuur, E. A. G., Abbott, B. W., Bowden, W. B., Brovkin, V., Camill, P., Canadell, J. G., et al. (2013). Expert assessment of vulnerability of permafrost carbon to climate change. *Climatic Change*, *119*(2), 359–374. https://doi.org/10.1007/s10584-013-0730-7

Schuur, E. A. G., Bockheim, J., Canadell, J. G., Euskirchen, E., Field, C. B., Goryachkin, S. V., et al. (2008). Vulnerability of permafrost carbon to climate change: Implications for the global carbon cycle. *Bioscience*, *58*(8), 701–714. https://doi.org/10.1641/B580807

Schuur, E. A. G., McGuire, A. D., Schädel, C., Grosse, G., Harden, J. W., Hayes, D. J., et al. (2015). Climate change and the permafrost carbon feedback. *Nature*, *520*(7546), 171–179. https://doi.org/10.1038/nature14338

Spencer, R. G. M., Aiken, G. R., Wickland, K. P., Striegl, R. G., & Hernes, P. J. (2008). Seasonal and spatial variability in dissolved organic matter quantity and composition from the Yukon River basin, Alaska. *Global Biogeochemical Cycles*, *22*, GB4002. https://doi.org/10.1029/2008GB003231

Spencer, R. G. M., Mann, P. J., Dittmar, T., Eglinton, T. I., McIntyre, C., Holmes, R. M., et al. (2015). Detecting the signature of permafrost thaw in Arctic rivers. *Geophysical Research Letters*, *42*, 2830–2835. https://doi.org/10.1002/2015GL063498

Striegl, R. G., Aiken, G. R., Dornblaser, M. M., Raymond, P. A., & Wickland, K. P. (2005). A decrease in discharge-normalized DOC export by the Yukon River during summer through autumn. *Geophysical Research Letters*, *32*, L21413. https://doi.org/10.1029/2005GL024413

Stubbins, A., Spencer, R. G. M., Chen, H., Hatcher, P. G., Mopper, K., Hernes, P. J., et al. (2010). Illuminated darkness: Molecular signatures of Congo River dissolved organic matter and its photochemical alteration as revealed by ultrahigh precision mass spectrometry. *Limnology and Oceanography*, *55*(4), 1467–1477. https://doi.org/10.4319/lo.2010.55.4.1467

Stuiver, M., & Polach, H. A. (1977). Discussion reporting of 14 C data. *Radiocarbon*, *19*(03), 355–363. https://doi.org/10.1017/S0033822200003672

Tarnocai, C., Canadell, J. G., Schuur, E. A. G., Kuhry, P., Mazhitova, G., & Zimov, S. (2009). Soil organic carbon pools in the northern circumpolar permafrost region. *Global Biogeochemical Cycles*, *23*, GB2023. https://doi.org/10.1029/2008GB003327

Throckmorton, H. M., Heikoop, J. M., Newman, B. D., Altmann, G. L., Conrad, M. S., Muss, J. D., et al. (2015). Pathways and transformations of dissolved methane and dissolved inorganic carbon in Arctic tundra watersheds: Evidence from analysis of stable isotopes. *Global Biogeochemical Cycles*, *29*, 1893–1910. https://doi.org/10.1002/2014GB005044

Vannote, R. L., Minshall, G. W., Cummins, K. W., Sedell, J. R., & Cushing, C. E. (1980). The river continuum concept. *Canadian Journal of Fisheries and Aquatic Sciences. Journal Canadien Des Sciences Halieutiques et Aquatiques*, *37*(1), 130–137.

Vonk, J. E., & Gustafsson, Ö. (2013). Permafrost-carbon complexities. *Nature Geoscience*, *6*(9), 675–676. https://doi.org/10.1038/ngeo1937

Vonk, J. E., Mann, P. J., Davydov, S., Davydova, A., Spencer, R. G. M., Schade, J., et al. (2013). High biolability of ancient permafrost carbon upon thaw. *Geophysical Research Letters*, *40*(11), 2689–2693. https://doi.org/10.1002/grl.50348

Vonk, J. E., Tank, S., Mann, P. J., Spencer, R., Treat, C., Striegl, R., et al. (2015). Biodegradability of dissolved organic carbon in permafrost soils and aquatic systems: A meta-analysis. *Biogeosciences*, *12*(23), 6915–6930. https://doi.org/10.5194/bg-12-6915-2015

Ward, C. P., & Cory, R. M. (2015). Chemical composition of dissolved organic matter draining permafrost soils. *Geochimica et Cosmochimica Acta*, *167*, 63–79. https://doi.org/10.1016/j.gca.2015.07.001

Ward, N. D., Keil, R. G., Medeiros, P. M., Brito, D. C., Cunha, A. C., Dittmar, T., et al. (2013). Degradation of terrestrially derived macromolecules in the Amazon River. *Nature Geoscience*, *6*(7).

Weishaar, J. L., Aiken, G. R., Bergamaschi, B. A., Fram, M. S., Fujii, R., & Mopper, K. (2003). Evaluation of specific ultraviolet absorbance as an indicator of the chemical composition and reactivity of dissolved organic carbon. *Environmental Science & Technology*, *37*(20), 4702–4708. https://doi.org/10.1021/es030360x

Zimov, S. A., Schuur, E. A. G., & Stuart Chapin, F. (2006). Permafrost and the global carbon budget. *Science*, *312*(5780), 1612–1613. https://doi.org/10.1126/science.1128908